Egypt. J. Chem. **Vol. 66**, No.SI 13. pp. 2219 - 2230 (2023)

Egyptian Journal of Chemistry

http://ejchem.journals.ekb.eg/

In-vivo Targeted Delivery of Doxorubicin Using Controlled In-situ Functionalized Chitosan Carbon Nanotubes: Possible Antitumor Effect.

Rasha F. Zahran[1*], Norhan A. Rezk[2] and El-Shahat A. Toson[3]

[1] Biochemistry Division, Chemistry Department, Faculty of Science, Damietta University, Egypt.

[2] Biochemistry Division, Chemistry Department, Faculty of Science, Damietta University, Egypt.

[3] Biochemistry Division, Chemistry Department, Faculty of Science, Damietta University, Egypt.

Abstract

Chitosan-wrapped multi-walled carbon nanotubes/Doxorubicin (CS-MWCNTs/DOX) nanoparticles were used to control delivery of doxorubicin into Ehrlich ascites carcinoma-bearing mice (EAC-bearing mice). Both CS-MWCNTS/DOX and free DOX were intraperitoneally injected into EAC-bearing mice. Tumor killing, animal survival, and changes in biochemical and apoptotic markers associated with cell growth or cell death were all assessed in *vivo*. The results demonstrated that, treatment of EAC-bearing mice with loaded and free DOX increased the animals' life span (49.3±2.5 and 40±3) compared to 17 days for the untreated tumor-bearing mice. Treating with CS-MWCNTs/DOX significally reduced cardiac enzymes compared to treating with free DOX. Furthermore, BAX and Caspase-3 levels as apoptotic markers were elevated in liver tissue homogenate, whereas Bcl-2 levels as anti-apoptotic marker were decreased. So, necrosis and apoptosis were the suggested mechanisms of tumor killing. Finally, the prepared drug delivery system succeeded to treat the tumor with reducing the free drug side effects.

Keywords: Multi-walled carbon nanotubes; Chitosan; Doxorubicin

1. Introduction

Cancer is among the leading causes of death. After heart illnesses, it is the second biggest cause of death globally [1]. One of the most effective cancer treatments is chemotherapeutic drugs. However, these agents cause severe adverse effects [2], which can be attributed to their ability to differentiate accurately between tumor and normal cells as Along with the tumour cells, they would also assault the body's normal tissue cells [3]. Among these agents is DOX, an anthracycline antibiotic with potent activity against solid tumors and hematological malignancies [4]. DOX's primary adverse effect is cardiotoxicity. Therefore, development of an effective carrier system for it can reduce its harmful effects.

Carbon nanotubes (CNTs) is one of these nano-carriers which attracted great interest because of its hollow tubular structure, ultrahigh surface area, and ability to penetrate membranes without causing cell damage. So, it attracted a significant interest for using in biomedical applications [5, 6, 7]. CNTs must be functionalized in order to establish them in possible medical applications and to combine them with biological systems [6]. In this study, CS-MWCNTs was used to deliver DOX to the tumor sites.

*Corresponding author e-mail: zahran@du.edu.eg.; (Rasha Fekry Zahran).
Received date 02 November 2022; revised date 16 May 2023; accepted date 30 May 2023
DOI: 10.21608/EJCHEM.2023.172022.7147

2. Materials and methods:

2.1. Materials

Readily-prepared CS-MWCNTs/DOX and DOX HCl (2mg/ml) was purchased from a local pharmacy. Alanine aminotransferase (ALT), aspartate aminotransferase (AST), albumin, creatinine, lactate dehydrogenase (LDH), and creatine kinase- MB (CKMB) kits were obtained from BIODIAGNOSTIC, Egypt. ELISA kits for BAX, Bcl-2, and caspase-3 were purchased from Elabscience Biotechnology Inc, USA.

2.2. Methods

2.2.1 Experimental animals

We employed 105 mature female Swiss albino mice, weighing 25 to 30 g on average, that were purchased from the National Cancer Institute in Cairo, Egypt. Mice were kept for two weeks in cages made of steel mesh prior to experimental use. The National Academy of Science created the "Guide for the Care and Use of Laboratory Animals," which was published by the National Institutes of Health. The animals were kept in a consistent environment with a 12:12 hour light/dark cycle, a temperature of 23+2 °C, and controlled humidity. They were given a conventional mouse pellet meal along with unlimited access to water.

2.2.2. Cell line

The parent Ehrlich ascites carcinoma (EAC) cell line was provided by Nile Center for Experimental Research (NCER), Mansoura, Egypt, and was used for in *vivo* study. The tumor cell line was preserved in mice through serial intraperitoneal (i.p.) transplantations of 1 x 10^6 viable tumor cells in 0.2 ml saline. The tumor is characterized by moderately speedy growth, which caused death of mice in 14 to 18 days due to the increase of ascitic fluid.

2.2.3. Induction of EAC liquid tumor

EAC cells were harvested 7-10 days after i.p. implantation. The collected cells were diluted with saline to obtain a concentration of 5 x 10^6 viable EAC cells per ml. A volume of 0.2 ml saline containing (1 x 10^6 EAC) was i.p. implanted into each normal mouse to induce EAC liquid tumor**.**

2.2.4. Experimental design:

Mice were divided into seven groups **(n=15).** These groups include healthy mice, healthy mice treated with CS-Ox-MWCNTs, and untreated EAC-bearing mice. The fourth and the fifth groups were tumorized mice treated i.p. with free DOX at a dose of 3 mg/kg and 1.5 mg/kg daily for two weeks. The sixth and seventh groups were EAC-bearing mice treated with CS-Ox-MWCNTs/DOX with doses equivalent to free DOX (3mg/kg) and (1.5mg/kg) daily for two weeks.

2.2.5. Evaluation of biological parameters after intraperitoneal (i.p.) administration

Twenty-four hours after the last dose, eight mice from each group were fasted for 8 hours. Then, they were weighed and sacrificed to evaluate serum biochemical parameters and hepatic antioxidative content. Blood samples were collected by cardiac puncture and were left to clot. Serum was separated using a cooling centrifuge (4°Cat 3000 rpm for 10 minutes). The separated sera were freshly used or frozen at -20°C until use.

Each mouse's liver was removed, rapidly rinsed with ice-cold PBS to remove blood, and dried on filter paper. Following drying, they were weighed. Using tissue homogenates prepared in ice-cold PBS (50 mM, pH 7.5), antioxidant parameters were determined.

The remaining animals were utilized for analyses of survival. Individual ascitic fluid samples were collected from untreated EAC-bearing mice and tumor-bearing mice treated with DOX in its free and loaded forms, their volumes were measured, and their viability was evaluated using the trypan blue exclusion method and a light microscope.

2.2.6. Estimations

2.2.6.1. Estimation of survival parameters

Mean survival time (MST) was determined according to the following formula: (MST= [day of the first death. + day of last death.]/2).

The percent of the increase in life span (%ILS) was calculated as the following: [(MST of treated group/MST of the EAC control group)-1] *100.

2.2.6.2. Estimation of immuno-chemical parameters:

Tumor necrosis factor (TNF-α), caspase-3, BAX, and Bcl-2 proteins levels were measured using commercially available assay kits. The activities of acid mammalian chitinase (AMCase) were also assessed following the method described by **Isaac and Gokhale (1982)** [8].

2.2.6.3. Estimation of biochemical parameters in serum and hepatic antioxidants levels in liver tissue:

Activities of LDH and creatine kinase –MB (CK-MB) were measured as indicators of cardiac functions, whereas creatinine and urea levels were assayed as indices of kidney functions. Finally, ALT, AST, and albumin levels were done as liver function tests. Reduced glutathione (GSH) level was measured using Ellman's reagent, levels of malonaldehyde (MDA), as a sign for lipid

peroxidation, super oxide dismutase (SOD) activity utilizing nitroblue tetrazolium mediated reduction of NBT, catalase (CAT) activity, and finally, nitric oxide (NO) concentrations were measured following the methods of **Beutler *et al.*, (1963)** [9]**, Buege and Aust (1978)** [10]**, Nishikimi *et al.* (1972)** [11]**, (Sinha,1972)** [12] **and Montgomery and Dymock (1961)** [13]**,** respectively.

2.2.7. Statistical analysis:

SPSS software (version 22) was used to analyze our data. All results were expressed as mean ± STD. The one-way ANOVA test was used to analyze the differences in means between the various treated groups and control. The level of statistical significance was set at $p < 0.05$.

3. Results and Discussion

3.1. Ascitic volume, cell viabilities, and survival parameters:

In the present study, the ascites fluids were withdrawn, and their volumes were determined. Viabilities and mortalities of the studied cells were also evaluated. Treatment of EAC-infected mice with free and loaded DOX at the higher dose (3 mg/kg) eradicates EAC and inhibits its growth. In contrast, after treatment with the lower dose (1.5 mg/kg), the ascitic volumes and cell viabilities were decreased (2.56±0.56 and 1.18±1.17 ml and 76.02±0.448 % and 35.32±22.88%) for free and loaded DOX, respectively (Figure 1, A).

Treatment of EAC-bearing mice with Ox-MWCNTs-CS/DOX at different doses significantly raised the MST from 15.8 to 31.5 days with a 94.11% increase in their life span (ILS) in case of lower dose treatment and from 15.8 to 49.3days with 203.5 % increase in the life span at the higher dose. Conversely, treating of EAC-bearing mice with the free DOX at a lower dose caused an increase in MST from 15.8 to 23.5days, with a 47 % increase in their life span. Similarly, the higher treatment dose increased the MST from 15.8 to 40 days with 147 % ILS (Table 1) (Figure 1, B). These results align with the in vitro cytotoxicity of MCF-7 cells which the loaded DOX has more tumor-killing effect than the free one.

These results can be attributed to the ability of CS-Ox-MWCNTs/ DOX for sustained release of more DOX at the tumor cell sites either via pH or thermo sensitivities or both [14], indicating effective inhibition of tumor growth via DOX-loading. These findings align with X. Qi et al. (2015) [15], who found that mice treated with DOX loaded on O-CNTs-LCH decreased tumor volumes compared to those treated with the free drug, showing a better in vivo intracellular DOX uptake. The increased uptake induced more tumor inhibitory effects of the loaded DOX.

Prolongation of life span is regarded as a reliable parameter for evaluating the efficacy and quality of any anticancer therapy. The previous results proved that DOX immobilization enhances its anti-tumor effect and reduces its toxicity. Similar results were obtained by Ma et al. (2018) [16], who used DOX loaded on nanographene oxide nanohybrids. The MST of the loaded DOX-treated mice was about two times longer than those treated with free DOX-treated one. Additionally, Hao et al. (2013) [17] demonstrated that nanoparticles loaded with DOX can decrease their toxicity and increase the MST of mice compared with free DOX. In addition, the study obtained by Li et al. (2016) [18], who used BSA-V-NPs to deliver DOX, indicates that these NPs loaded DOX were more effective than the corresponding free DOX, at least in part on the level of increasing their lifespan of the tumor-bearing mice.

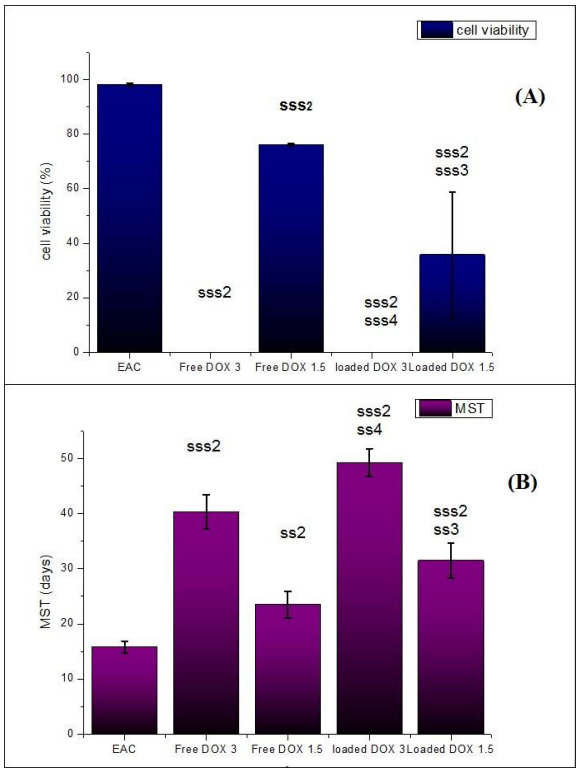

Figure1: Cell viabilities (A) and mean survival time (B) of EAC treated groups. Each bar represens as mean±STD (n=8). Asterisks (s,ss,sss) indicates P<0.05, 0.01, 0.001 and (n) not significant vs 1 healthy control, 2 EAC control, 3 free DOX 1.5mg/kg, 4 free DOX 3 mg/kg

3.2. Change in biochemical Parameters in tissue homogenate and serum:

3.2.1. Immuno-chemical parameters

Apoptosis (programmed cell death) is regulated by some molecular markers. These factors involved a network of genes and proteins, which play a significant role in this process [19]. Among these markers, BAX, caspase-3, and Bcl-2 were measured in this study using the ELISA technique. The levels of TNF-, BAX, BCl-2, and caspase-3 proteins, as well as the activity of AMCase, were substantially higher in EAC-inoculated mice than in healthy mice. TNF-, BAX, and caspase-3 levels increased after treatment, while AMCase activity decreased significantly in a dose-dependent manner, particularly in mice treated with loaded DOX. (Table 2,3) (Figure 2).

BAX is a Bcl-2-related multi-domain pro-apoptotic protein that promotes apoptosis in cultured cells [20,21]. Caspase-3 is a main mediator of apoptosis via which cell apoptosis is regulated. Activation of caspase-3 stimulates the subsequent stages of apoptosis, including protein degradation, membrane damage, and DNA cleavage [22]. In contrast, Bcl-2 protein acts as an anti-apoptotic activator by inhibiting cytochrome C's liberation from mitochondria [23]. From the previous result, one can suggest that the decrease of Bcl-2 cause pores formation in the mitochondrial membrane. Such perforation mediates the release of cytochrome C and pro-caspase-9, mediating caspase-3-dependent apoptosis [24]. Therefore, it is hypothesized that the loaded DOX concentrated at the tumor site and its controlled release enhanced the apoptotic process mainly by elevating caspase-3, BAX and/or inhibiting Bcl-2. These results are consistent with Abdel-Hakeem et al. (2020) [25], who found that treatment of MDA-MD-231 breast cancer cell line with DOX loaded on the CS nanoparticles had resulted in a more significant decrease in the level of Bcl-2 protein compared to those which were treated with the free DOX.

TNF-α is a crucial protein for the normal immune response to infection, but excessive amounts are harmful as this protein mediates the generation of excessive reactive oxygen species (ROS) [26]. It had been shown that the key survival factor, NF-κB stimuli ROS-neutralizing enzymes like superoxide dismutase. Stimulus of ROS production or inhibition of the NF-κB pathway by cyclooxygenase-2 (COX-2) inhibitors has confirmed to be successful in alerting tumor cells to TNF-α–prompted apoptosis [27]. As previously demonstrated, TNF-alpha can promote apoptosis in a dose- and time-dependent way explains its elevation. In high therapeutic doses, TNF-alpha can disrupt tissue vasculature, increasing vascular permeability and thus help accumulate the chemotherapeutic agents at the site of tumor growth [28]. The increase in the level of pro-inflammatory cytokines, TNF-α, after DOX administration, induces severe inflammatory responses in the liver and various organs, in addition to its well-known cardiac toxicity [29].

These results are compatible with the results obtained by Keeney et al. (2018) [30], who found that DOX administration led to increased levels of TNF-α and oxidative stress in the brain. Furthermore, Wang et al. (2016) [29] found that the level of TNF-α in DOX-treated patients was significantly higher than in Dox-untreated patients.

AMCase was the second chitinase identified and is mainly expressed in the stomach and, to a lesser extent, in the lung. It is stable at a highly acid pH [31], a member of the 18-glycosidase family, and is expressed in epithelial cells and specific immune cells (such as macrophages and neutrophils) in different organs [32].

The activity of this enzyme in liver tissue homogenate of untreated EAC-inoculated mice was elevated. This finding may be mainly due to the ability of DOX to produce free radicals, which lead to the induction of inflammatory mediators, containing inducible nitric oxide synthase (iNOS) and Cyclooxygenase-2 (COS-2), which contribute to cancer invasiveness by activating several matrix metalloproteinases [33, 34].

In contrast, the same enzyme activity was significantly reduced in the treated mice with loaded DOX compared to those treated with the free one. This is mainly because of enhanced CNTs-drug internalization and/or cancer cells-pH sensitive free drug release accumulation with a resultant decrease in normal tissue DOX concentration. These results were similar to that of Aljobaily et al. (2021) [35], who found that DOX can cause acute inflammation by r the production of inflammatory cytokines such as TNF-α, IL-1β; which are simulants of free radical formation. A combined DOX entrapment protocol may contribute to the treatment of tumors by simultaneously lowering the normal cytotoxicity of normal cells.

These findings align with Lee et al. (2020) [19], who found that the delivery of DOX using glycol CS nanoparticles can significantly decrease COX-2 activity and nuclear factor kappa B (NF-ϰB) level than free DOX using the murine A549-Luc xenograft mice.

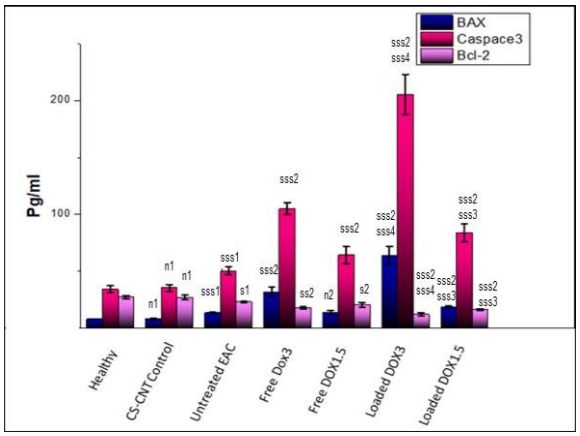

Figure 2: Mean levels of apoptotic proteins (BAX, Caspase 3 and Bcl-2) in different groups. Each bar represents as mean±STD (n=8). Asterisks (s,ss,sss) indicates P<0.05, 0.01, 0.001 and (n) not significant vs 1 healthy control, 2 EAC control, 3 free DOX 1.5mg/kg, 4 free DOX 3 mg/kg

3.2.2. Markers of antioxidative stress and biochemical parameters in serum

The main levels of MDA and NO were significantly increased in the liver tissue homogenate of the untreated EAC-bearing mice compared to those of healthy ones. On the other hand, the levels of antioxidants, including GSH, CAT, and SOD, were significantly decreased versus those after treatment with both free and loaded DOX. Compared to free DOX, treatment with the loaded one significantly lower the oxidative stress (Table2 and 4).

The mean serum activities of ALT, AST, LDH, and CK-MB and the levels of both creatinine and urea were increased in EAC-inoculated mice compared to those of the healthy. Conversely, the albumin level was significantly decreased in EAC untreated mice compared to the healthy group. These results indicate liver, heart, and kidney damage.

Generally, treatment of mice bearing EAC with free or loaded DOX induced significant decreases in the activities of both ALT and AST and the levels of both creatinine and urea compared with the untreated tumor-bearing mice. Conversely, the serum albumin level was increased compared to those of the EAC-inoculated mice. Similarly, the activities of both LDH and CK-MB, as markers of heart damage, were more elevated in a dose-dependent manner. As hypothesized, if the loaded DOX results were compared with the corresponding values of a free one, liver, kidney, and heart functions were enhanced (Table 6), Figure 3.

DOX treatment has a significant adverse effect on cardiotoxicity. Therefore, it is necessary to investigate the potential safety profile of the DOX-loaded nanocarrier in relation to its cardiotoxicity. The current study findings revealed that increased cardiac enzymes induced organ damage. Hajra et al. (2018) [36] speculated that the oxidative stress-mediated mechanism as reported by Zhang et al. (2021) [37]. Similar results were reported by Rita et al. (2018) [38], who found that the administration of free DOX at a dose of 3-6 mg/kg resulted in a slight elevation in serum LDH and CK-MB activities.

These adverse effects were mitigated by the prolonged release of DOX from its nanocarrier in response to the pH of the tumor site. Similarly, the study by Durairaj et al. (2022) [39] showed that the delivery of DOX by CS nanoparticles could decrease the elevation of LDH and CK-MB enzymes and reduce cardiotoxicity. Also, the study obtained by El-Ashmawy et al. (2017) [40] showed that the loading of DOX on Poly-N-acetyl glucosamine nanoparticles could effectively decrease cardiotoxicity and cause fewer side effects without decreasing the drug efficacy compared with its free form.

DOX can adversely affect the myocardium and significantly damage the liver with a consequent increase in serum transaminase activities [41] because DOX, like many other drugs, is mainly concentrated in the liver, the primary site of drug metabolism. This compartmentalization can induce hepatotoxicity [42]. Moreover, DOX can alternate hepatic redox status because the quinone structure of DOX is converted into semi-quinone radicals, whereas the latter radicals react with oxygen and rapidly produce superoxide anion, a substrate of SOD dismutation which can be converted into hydrogen peroxide [43]. In the presence of catalase, H2O2 is converted to O2 and water. In contrast, the generated H2O2 undergoes homological fission into 2 -OH, which is more effective than the parent molecule (H2O2) in the absence of CAT or (decrease of its activity as in tumor) [40], which mainly occurs following free DOX treatment. The redox status involvement in DOX hepatotoxicity was early reported by Donia et al. (2018) [44]. Unfortunately, the activities of catalase and superoxide dismutase enzymes and the level of GSH were substantially inhibited or consumed in the hepatic tissues in the EAC untreated mice and free DOX treated mice compared to healthy control mice.

Table 1: Effect of different treatments on Tumor volume, cell viability, mean survival time (MST) and percent of increase in life span (ILS).

Groups	Ascitic volume (ml)	Total NO. of viable cells ($\times 10^9$)	Cell viability (%)	MST (days)	ILS (%)
EAC control	10.53±1.18	2.37±0.3	98.2±0.53	15.8±1.1	-------
EAC+free DOX 3mg/kg	0	0	0	40±3.1	147
EAC+free DOX 1.5mg/kg	2.56±0.56^{sss2}	0.387±0.086^{sss2}	76.02±0.44^{sss2}	23.5±2.4	47
EAC+loaded DOX 3mg/kg	0	0	0	49.3±2.5	203.5
EAC+loaded DOX 1.5mg/kg	1.18±1.17^{sss2,ss3}	0.0268±0.027^{sss2,sss3}	35.8±22.8^{sss2,sss3}	31.5±3.2	94.11

Data are represented as mean±STD (n=8). Asterisks (^{s},^{ss},^{sss}) indicates P<0.05, 0.01, 0.001 and (^{n}) not significant vs [1] healthy control, [2] EAC control, [3] free DOX 1.5mg/kg, [4] free DOX 3 mg/kg.

Table 2: Effect of tumor inoculations and treatments on the mean activity of AMCase and the mean concentrations of TNF-α and NO.

Groups	TNF-α (ng/ml)	AMCase (U/l)	NO (µmol/l)
Healthy control	2.92±0.255	9.95±2.4	8.74±1.34
CS-Ox-MWCNTs control	2.8±0.33^{n1}	10.6±2^{n1}	10.86±1.16^{s1}
EAC control	6.84±1.03^{sss1}	31.84±2.23^{sss1}	38.11±4.13^{sss1}
EAC+free DOX 3mg/kg	12.192^{sss2}	25.3±3.6^{ss2}	28.22±3.5^{sss2}
EAC+free DOX 1.5mg/kg	7.1±0.88^{s2}	25.84±1.84^{ss2}	25.44±2.7^{sss2}
EAC+loaded DOX 3mg/kg	20.48±2.26^{sss2,sss4}	14.44±2.8^{sss2,sss4}	24.36±1.78^{sss2,s4}
EAC+loaded DOX 1.5mg/kg	8.62±1.1^{ss2,ss3}	19.11±2.29^{sss2,sss3}	31.07±1.82^{ss2,sss3}

Table 3: Effect of tumor inoculations and treatments on the mean concentrations of BAX, Bcl-2 and Caspase3 in different groups.

Groups	BAX (pg/ml)	Caspase3 (pg/ml)	Bcl-2 (pg/ml)
Healthy control	7.9±1	34.09±2.96	27.28±1.44
CS-Ox-MWCNTs control	8.02 ± 0.64^{n1}	35 ± 3.1^{n1}	26.86 ± 2.03^{n1}
EAC control	13.4 ± 0.97^{sss1}	50.4 ± 3.23^{sss1}	23.02 ± 0.63^{s1}
EAC+free DOX 3mg/kg	31.86 ± 4.16^{sss2}	104.9 ± 5.18^{sss2}	17.72 ± 1.2^{ss2}
EAC+free DOX 1.5mg/kg	13.75 ± 1.64^{n2}	64.23 ± 7.39^{sss2}	20.4 ± 2.14^{s2}
EAC+loaded DOX 3mg/kg	$63.86\pm7.75^{sss2,sss4}$	$205.4\pm17.5^{sss2,sss4}$	$12.23\pm1.44^{sss2,sss4}$
EAC+loaded DOX 1.5mg/kg	$18.71\pm0.67^{sss2,sss3}$	$83.62\pm7.93^{sss2,sss3}$	$16.05\pm0.96^{sss2,sss3}$

Table 4: Effect of tumor inoculation and treatments on the activity of Catalase, the mean level of GSH and MDA and percent of inhibition of SOD.

Groups	Catalase (U/l)	SOD inhibition (%)	GSH (µmol/l)	MDA (nmol/l)
Healthy control	3.05±0.59	83.28±5.2	40.5±2.28	53.27±8.01
CS-Ox-MWCNTs control	3.18 ± 0.59^{n1}	80.13 ± 2.37^{n1}	36.97 ± 3.33^{s1}	49.8 ± 4.68^{n1}
EAC control	0.43 ± 0.034^{sss1}	34.95 ± 3.7^{sss1}	20.02 ± 3.05^{sss1}	398 ± 34.32^{sss1}
EAC+free DOX 3mg/kg	0.77 ± 0.03^{sss2}	58.52 ± 3.6^{sss2}	28.5 ± 4.46^{sss2}	326.3 ± 33.46^{ss2}
EAC+free DOX 1.5mg/kg	0.9 ± 0.082^{sss2}	49.08 ± 5.06^{sss2}	29.76 ± 2.02^{sss2}	157.45 ± 14.53^{sss2}
EAC+loaded DOX 3mg/kg	$1.11\pm0.12^{sss2,sss4}$	$70.8\pm4.5^{sss2,sss4}$	$35.07\pm3.9^{sss2,sss4}$	$249.36\pm1.78^{ss2,sss4}$
EAC+loaded DOX 1.5mg/kg	$1.05\pm0.087^{sss2,ss3}$	$61.6\pm1.76^{sss2,sss3}$	$34.22\pm2.48^{sss2,sss3}$	$116.63\pm12.8^{sss2,sss3}$

Table 5: The effect of tumor inoculation and treatments on the mean activities of ALT, AST and the mean levels of serum albumin.

Groups	ALT (U/l)	AST (U/l)	Albumin (g%)
Healthy control	29.75±3.84	68.42±5.31	4.8±0.207
CS-Ox-MWCNTs control	26.75±2.2^{n1}	64.85±8.15^{n1}	4.54±0.33^{n1}
EAC control	62.2±4.88^{sss1}	114.79±4.46^{sss1}	3.1±0.18^{sss1}
EAC+free DOX 3mg/kg	64.79±5.7^{n2}	100.64±6.13^{ss2}	3.54±0.23^{s1}
EAC+free DOX 1.5mg/kg	108±2.5^{sss2}	113.9±40.51^{n2}	3.22±0.08^{n2}
EAC+loaded DOX 3mg/kg	55.77±2.26^{ss2,ss4}	94.37±6.5^{sss2}	3.87±0.09^{ss2,ss4}
EAC+loaded DOX 1.5mg/kg	77.56±5.3^{ss2,sss3}	97.3±7.6^{sss2}	3.79±0.24^{ss2,sss3}

Table 6: The effect of tumor inoculation and treatments on the mean activities of LDH and CK-MB and the mean levels of serum creatinine and urea.

Groups	CK-MB (U/l)	LDH (U/l)	Creatinine (mg%)	Urea (mg%)
Healthy control	96.45±4.06	209.9±9.3	0.557±0.08	44.44±3.7
CS-Ox-MWCNTs control	107±5.3^{s1}	221±7.3^{s1}	0.606±0.06^{n1}	41.3±1.8^{n1}
EAC control	242±6.2^{sss1}	411.5±4.46^{sss1}	1.6±0.14^{sss1}	63.9±4^{sss1}
EAC+free DOX 3mg/kg	595.5±15.87^{sss2}	896.5±17.51^{sss2}	0.993±0.097^{ss2}	70.3±4.3^{ss2}
EAC+free DOX 1.5mg/kg	374.7±21.5^{sss2}	779.2±40.7^{sss2}	0.94±0.12^{ss2}	63.8±2.8^{n2}
EAC+loaded DOX 3mg/kg	314.66±9.47^{sss2,sss4}	597.4±15.6^{sss2,sss4}	0.84±0.076^{sss2,ss4}	45.8±2.8^{sss2,sss4}
EAC+loaded DOX 1.5mg/kg	269±18.83^{ss2,sss3}	471.6±15.6^{sss2,sss3}	0.74±0.086^{sss2,ss3}	54.9±3^{sss2,sss3}

Data are represented as mean±STD (n=8). Asterisks (^{s},^{ss},^{sss}) indicates P<0.05, 0.01, 0.001 and (^{n}) not significant vs [1] healthy control, [2] EAC control, [3] free DOX 1.5mg/kg, [4] free DOX 3 mg/kg.

Therefore, the continual decrease in the activities of SOD and CAT, as well as reduction of GSH during tumor progression or DOX compartmentalization in the liver, mediate hepatic disorder with a resultant increase in its enzyme activity and reduction in its albumin level.

They collaboratively mediate MDA and NO accumulation in hepatic tissue, which necessitates the presence of a state of oxidative stress following DOX treatment and tumor cell metastasis, as evidenced by the findings of the current study [45]. In this regard, this metastasis stimulates the production of ROS by the cancer cells more than by normal cells [46].

The significant decrease in the hepatic glutathione reduced (GSH) level and the SOD and catalase activities in EAC inoculated mice, and DOX treated mice and their re-elevation after targeted delivery of DOX using CNTs confirm the potential use of such delivery technique to reduce organ toxicity, including the liver. Furthermore, this targeted delivery technique caused a significant decrease in MDA and NO levels in hepatic tissue compared to untreated EAC inoculated mice and free DOX-treated mice. These results are consistent with El-Ashmawy et al. (2018) [46], who found that the treatment of mice with free DOX showed a significant decrease in SOD and CAT levels compared to tumor control. On the contrary, the mice group treated with DOX loaded on an F2 gel composite matrix harbored a significant increase of antioxidant enzymes, in addition to the effect of EAC metastasis into the liver [33].

The kidney is a sensitive organ most frequently affected by any toxic compound. Chemotherapy treatments may cause kidney damage, resulting in acute kidney failure [47]. The behavior of free DOX and EAC metastasis is the same as that of the liver. In this regard, nephrotoxicity was observed [48]. After DOX entrapment, the nephrotoxic effects were reduced (serum urea and creatinine levels were decreased). This finding may be due to the reduction of oxidative stress on vital organs, including the kidney, via the targeted delivery, controlled release of DOX in the tumor sites, and reduction in tumor metastasis or both [49]. These results are consistent with Yang et al. (2017) [50], who studied the biodistribution of DOX encapsulation pH triggered CS nanogel using hepatocellular carcinoma-bearing mice and showed that the DOX concentration was substantially lower in heart, lung, and kidney in case of loaded DOX than that of the free DOX.

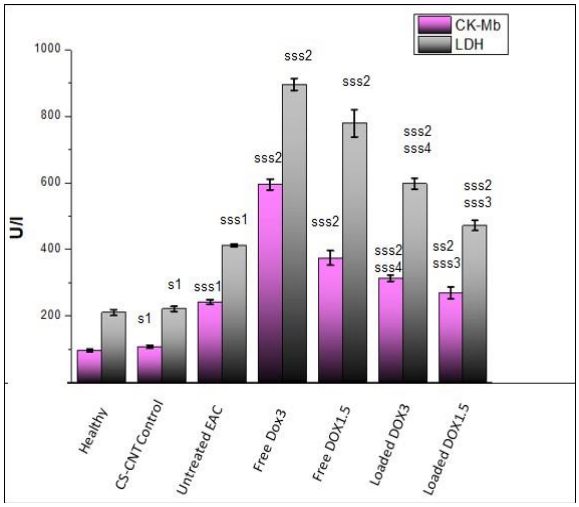

Figure 3: Mean activities of cardiac enzymes (CK-Mb and LDH) in different groups. Each bar represents as mean±STD (n=8). Asterisks (s,ss,sss) indicates P<0.05, 0.01, 0.001 and (n) not significant vs 1 healthy control, 2 EAC control, 3 free DOX 1.5mg/kg, 4 free DOX 3 mg/kg

4. Conclusion:

The previously prepared CS-MWCNTs/DOX successfully reduced cardiac and other organ damage and mediating tumor killing via inducing the pro-apoptotic proteins, namely caspase-3 and BAX, and reducing the production of the Bcl-2, as an anti-apoptotic protein.

Declaration of competing interest:

The authors declare that they have no known competing financial interests or personal relationships that could have appeared to influence the work reported in this paper.

Funding:

This research did not receive any specific grant from funding agencies in the public, commercial, or not-for-profit sectors.

References:

[1] Zaorsky, N. G., Churilla, T. M., Egleston, B. L., Fisher, S. G., Ridge, J. A., Horwitz, E. M. & Meyer,J. E. Causes of death among cancer patients. Annals of Oncology (2017) 28: 400–407. doi:10.1093/annonc/mdw604

[2] WANG, J.-J., LEI, K.-F., & HAN, F. Tumor microenvironment: recent advances in various cancer treatments. European Review for Medical and Pharmacological Sciences, (2018) 22: 3855-3864 doi: 10.26355/eurrev_201806_15270.

[3] Rivankar: doxorubicin formulations in cancer therapy, Journal of Cancer Research and

Therapeutics -(2014) Volume 10 - Issue 4 DOI: 10.4103/0973-1482.139267

[4] Makwana, V., Karanjia, J., Haselhorst, T., Anoopkumar-Dukie, S., & Rudrawar, S.. Liposomal doxorubicin as targeted delivery platform: Current trends in surface functionalization. International Journal of Pharmaceutics, (2021) 593(Jan), 120117. Doi: 10.1016/j.ijpharm.2020.120117

[5] Qi1, X., Rui1, Y., Fan,Y., Chen, H., Ma,N., Wu, Z.. Galactosylated chitosan-grafted multiwall carbon nanotubes forpH-dependent sustained release and hepatic tumor-targeted deliveryof doxorubicin in vivo. Colloids and Surfaces B: Biointerfaces (2015) 133, 314–322 http://dx.doi.org/10.1016/j.colsurfb.2015.06.003

[6] Sireesha,M., Babu, V. ., Ramakrishna, S. Functionalized carbon nanotubes in bio-world: Applications, limitations and future directions. Materials Science and Engineering B 223 (2017) 43–63 http://dx.doi.org/10.1016/j.mseb.2017.06.002

[7] Elhissi, A.M. A., Ahmed W., Hassan, I. Ul, Dhanak, V. R. and D'Emanuele1, A. Carbon Nanotubes in Cancer Therapy and Drug Delivery. Journal of Drug Delivery Volume 2012, Article ID 837327, 10 pages doi:10.1155/2012/837327

[8] Issac, S., & Gokhale, A. V. Autolysis: A tool for protoplastproduction from Aspergillus nidulans. Transactions of the British Mycological Society, (1982) 78(3), 389-394. Doi: 10.1016/S0007-1536(82)80147-2

[9] Beutler, E., Duron, O., &Kelly, B. M. Improved Methods for Determination of Blood Glutathione. Journal of Laboratory Clinics Medicine, (1963) 61(May),882-888 PMID: 13967893.

[10] Buege, J.A., & Aust, S. D. Microsomal lipid peroxidation. Methods in Enzymology, (1978) 52, 302-310. Doi: 10.1016/s0076-6879(78)52032-6

[11] Nishikimi, M., Appaji Rao, N., & Yagi, K. The occurrence of Superoxide anion in the reaction of reduced phenazine methosulfate and molecular oxygen. Biochemical and Biophysical Research Communications, (1972) 46(2), 849-854. Doi: 10.1016/S0006-291X (72)80218-3

[12] Sinha, A. K. Colorimetric assay of catalase. Analytical Biochemistry, (1972) 47(2), 389-394. Doi: 10.1016/0003-2697(72)90132-7

[13] Montgomery, H.A.C. and Dymock, J. (1961) The determination of nitrite in water. Analyst, 86, 414-416.

[14] Chatterjee, S., Hui, P. C. leung, Siu, W. S., Kan, c. Wai, Leung, P. C., Wanxue, C., & Chiou, J. C. Influence of pH-responsive compounds synthesized from chitosan and hyaluronic acid on dual-responsive (pH/tempreture) hydrogel drug delivery systems of Cortex Moutan. International Journal of Biological Macromolecules, 168(Jan), (2021)163-174. Doi: 10.1016/j.ijbiomac.2020.12.035

[15] Qi, X., Rui, Y., Fan, Y., Chen, H., Ma, N., Wu, Z. Galactosylated chitosan-grafted multiwall carbon nanotubes for pH-dependent sustained release and hepatic tumor-targeted delivery of doxorubicin in vivo. Journal of Colloids and Surfaces B: Biointerfaces 133, (2015) 314–322 http://dx.doi.org/10.1016/j.colsurfb.2015.06.003

[16] Ma, K., Fu, D., Liu, Y., Dai, R., Yu, D., Guo, Z., cui, C., Wang, L., Xu, J., & Mao, C. Cancer cell targeting, controlled drug release and intracellular fate of biomimetic membrane-encapsulated drug-loaded nano-graphene oxide nanohybrids. Journal of Materials Chemistry B, 6(31), (2018) 5080-5090. Doi: 10.1039/c8tb00804c

[17] Hao, H., Ma, Q., Huang, C., He, F., & Yao, P. Preparation, characterization, and in vivo evaluation of doxorubicin loaded BSA nanoparticles with folic acid modified dextran surface. International Journal of Pharmaceutics, 444(1-2), (2013)77-84. Doi: 10.1016/j.ijpharm.2013.01.041

[18] Li, F., Zheng, C., Xin,J., Chen,F., Ling,H., Sun,L., Webster,T. J., Ming,X., Liu, J. Enhanced tumor delivery and antitumor response of doxorubicin-loaded albumin nanoparticles formulated based on a Schiff base. International Journal of Nanomedicine 11(2016)3875–3890 http://dx.doi.org/10.2147/IJN.S108689

[19] Lee, R., Choi, Y. J., Jeong, M. S., Park, Y. IL, Motooyama, K., Kim, M. W., Kwon, S. H., & Choi, J. H. Halyuronic Acid-Decorated Glycol Chitosan Nanoparticles for pH-Sensetive Controlled Release of Doxorubicin and Celecoxib in Nonsmall Cell Lung Cancer. Bioconjugate Chemistry, 31(3), (2020) 923-932. Doi: 10.1021/acs.bioconjchem.0c00048

[20] Pistrillo, G., Trisciuoglio, D., D., Ceci, C., Alessia Garufi, & D'Orazi, G. Apatosis as anticancer mechanism: Function and dysfunction of its modulators and targeted therapeutic strategies. Aging, 8(4) (2016) 603-619. Doi: 10.18632/aging.100934

[21] Lalier, L., Franc¸ P., Cartron, O., Juin, P., Nedelkina, S., Manon, S., Bechinger, B., Vallette, F. M. Bax activation and mitochondrial insertion during apoptosis. Apoptosis (2007) 12:887–896 DOI 10.1007/s10495-007-0749-1

[22] Bader El-Din, N. K., Ali, D. A., & Abou-El-Magd, R.F. Grape seeds and skin induce tumor

growth inhibition via G1-phase arrest and apoptosis in mice inoculated with Ehrlich ascites carcinoma. Nutrition, 58(Feb), (2019) 100-109. Doi: 10.1016/j.nut.2018.06.018

[23] Yan, Jianqin, Chen, J., Zhang, N., Yang, Y., Zhu, W., Li, L., & He, B. Mitochondrial-targeted tetrahedral DNA nanostructures for doxorubicin delivery and enhancement of apoptosis. Journal of Materials Chemistry. B, 8(3), (2020)492-503. Doi: 10.1039/c9tb02266j

[24] Ramasamy, T., Ruttala, H. B., Sundaramoorthy, P., Poudel, B. K., Youn, Y. S., Ku, S. K., Choi, H.-G., Yong, C. S., & Kim, J.O. (2018). Multimodel selenium nanoshell-capped Au@mSiO2 nanoplatform for NIR-responsive chemo-photothermal therapy against metastatic breast cancer. NPG Asia Materials, 10(4), 197-216. Doi: 10.1038/s41427-018-0034-5

[25] M.A. Abd-Elhakeem, O.M. Abdel-Haseb, S.E. Abdel-Ghany, E. Cevik, H. Sabit, Doxorubicin loaded on chitosan-protamine nanoparticles triggers apoptosis via downregulating Bcl-2 in breast cancer cells, Journal of Drug Delivery Science and Technology (2019), doi: https://doi.org/10.1016/j.jddst.2019.101423

[26] Bradley, JR. TNF-mediated inflammatory disease. Journal of Pathology J Pathol 214: (2008)149–160 DOI: 10.1002/path.2287

[27] Horssen, R. V., Hagen, Timo L. M., Eggermont, A. M. M. TNF-α in Cancer Treatment: Molecular Insights, Antitumor Effects, and Clinical Utility. The Oncologist 2006;11:397–408 https://doi.org/10.1634/theoncologist.11-4-397

[28] Sharifa, P. M., Jabbaria, P., Razia, S., Fathia, M. K., Rezaeid,N. Importance of TNF-alpha and its alterations in the development of cancers. Cytokine 130 (2020) 155066 https://doi.org/10.1016/j.cyto.2020.155066

[29] Wang,Z. Q., Chen, M. T., Zhang, R., Zhang, Y., Li, W., and Li, Y. G. Docosahexaenoic Acid Attenuates Doxorubicin-induced Cytotoxicity and Inflammation by Suppressing NF-kB/iNOS/NO Signaling Pathway Activation in H9C2 Cardiac Cells. J Cardiovasc Pharmacol Volume 67, Number 4, April 20 (2016). doi: 10.1097/FJC.0000000000000350

[30] Keeney, J. T. R., Ren, X., Warrier, J., Noel, T., Powell, D. K., Brelsfoard, J. M., Sultana, R., Saatman, K. E., Clair, D. K. St., and Butterfield, D. A. Doxorubicin-induced elevated oxidative stress and neurochemical alterations in brain and cognitive decline: protection by MESNA and insights into mechanisms of chemotherapy-induced cognitive impairment ("chemobrain"). Oncotarget, 2018, Vol. 9, (No. 54), pp: 30324-30339 doi: 10.18632/oncotarget.25718

[31] Pinteac, R., Montalban, X., and Comabella, M. Chitinases and chitinase-like proteins as biomarkers in neurologic disorders. Neurol Neuroimmunol Neuroinflamm 2021;8: e921. doi:10.1212/NXI.0000000000000921

[32] Hu, c., Ma, Z., Zhu, J., Fan, Y., Tuo, B., Li, T., Liu, X. Physiological and pathophysiological roles of acidic mammalian chitinase (CHIA) in multiple organs. Biomedicine & Pharmacotherapy 138 (2021) 111465 https://doi.org/10.1016/j.biopha.2021.111465

[33] Adham, A. N., Abdelfatah, S., Naqishbandi, A. M., Mahmoud, N., & Efferth, T. Cytotoxocity of apigenin towards multiple myeloma cell lines and suppression of iNOS and COX-2 expression in STAT1-transfected HEK293 cells. Phytomedicine, 80(Jan), (2021)153371. Doi: 10.1016/j.phymed.2020.153371

[34] Burridge, P. W., & Thorp, E. B. Doxorubicin-induced ascension of resident cardiac macrophages. Circulation Research, 127(5), (2020)628-630. Doi: 10.1161/CIRCRESAHA.120.317626

[35] Aljobaily, N., Viereckl, M. J., Hydock, D. S., Aljobaily, H., Wu, T. Y., Busekrus, R., Jones, B., Alberson, J., & Han, Y. Creatine alleviates doxorubicin-induced liver damage by inhibiting liver fibrosis, inflammation, oxidative stress, and cellular senescence. In Nutrients (Vol.13, Issue 1, (2021) pp.41-55). Doi: 10.3390/nu13010041

[36] Hajra, S., Patra, A. R., Basu, A., Saha, P., & Bhattachharya, S. Indole-3-Carbinol (I3C) enhances the sensitivity of murine breast adenocarcinoma cells to doxorubicin (DOX) through inhibition of NF-ϰβ blocking angiogenesis and regulation of mitochondrial apoptotic pathway. Chemico-Biological Interactions, 290(June), (2018) 19-36. Doi: 10.1016/j.cbi.2018.05.005

[37] Zhang, Heping, Fan, L., Liao, H., Tu, L., Zhang, J., Xu, D. & Feng, J. Correlations of cardiac function with inflammation, oxidative stress and anemia in patients with uremia. EXP Ther Med, 21(3), 250. (2021) Doi: 10.3892/etm.2021.9681

[38] Zilinyi, R., Czompa, A., Czegledi, A., Gajtko, A., Pituk, D., Lekli, I., and Tosaki, A. The Cardioprotective Effect of Metformin in Doxorubicin-Induced Cardiotoxicity: The Role of Autophagy. Journal of Molecules 23, 1184; (2018) doi:10.3390/molecules23051184

[39] Siva, D., Abinaya, S., Rajesh, D., Archunan, G., Padmanabhan, P., Gulyás, P., and Achiraman, S. Mollification of Doxorubicin (DOX)-Mediated Cardiotoxicity Using Conjugated Chitosan Nanoparticles with Supplementation of Propionic Acid. Journal of Nanomaterials 12,

502. (2022) https://doi.org/10.3390/nano12030502

[40] El-Ashmawy, N. E., Khedr, E. G., Ebeid, E. Z. M., Salem, M. L., Zidan, A. A. A., & Mosalam, E.M. Enhanced anticancer effect and reduced toxicity of doxorubicin in combination with thymoquinone released from Poly-N-acetyl glucosamine nanomatrix in mice bearing solid Ehrlish carcinoma. European Journal of Pharmaceutical Sciences, 109(Sep), (2017)525-532. Doi: 10.1016/j.ejps.2017.09.012

[41] Rašković, A., Stilinović ,N., Kolarović, J., Vasović, V., Vukmirović, S., and Mikov, M. The Protective Effects of Silymarin against Doxorubicin-Induced Cardiotoxicity and Hepatotoxicity in Rats. Journal of Molecules 16, (2011)8601-8613; doi:10.3390/molecules16108601

[42] Elbialy, N. S., Fathy, M. M., & Khalil, W. M. Doxorubicin loaded magnetic gold nanoparticles for in vivo targeted drug delivery. International Journal of Pharmaceutics, 490(1-2), (2015)190-199. Doi: 10.1016/j.ijpharm.2015.05.032

[43] Tsutsui, A., Morishita, Y., Furumachi, H., Fujimoto, T., Hirai, R., Fujita, T., & Machinami, T. Generation of cyclic glutathione via the thiolactonization of glutathione and identification of a new radical scavenging mechanism. Tetrahedron Letters, 68(March), 152836. (2021) Doi: https://doi.org/10.1016/j.tetlet.2021.152836

[44] Donia, T. I. K., Gerges, M. N., & Mohamed, T. M. Amelioration effect of Egyptian sweet orange hesperidin on Ehrlich ascites carcinoma (EAC) bearing mice. Chemico-Biological Interactions, 285(April), (2018)76-84. Doi: 10.1016/j.cbi.2018.02.029

[45] Toson, E.-S. A., Almutairi, F. M., Elfalal, A. A., Habib, S. A., Zahran, R. F., & Elbakry, M. Suppression Effect of Superoxide Dismutase (SOD)-Like Activity Protein Partially Purified from Raphnus sativus Leaves against Liver Metastasis in Mice Intraperitoneally Infected with Ehrlich Ascites Carcinoma Cell. Natural Science, 2016, 8, 321-332. DOI: 10.4236/ns.2016.87037

[46] El-Ashmawy, N. E., Khedr, E. G., Ebeid, E. M., Salem, M. L.,Mosalam, E. M., Zidan, A. A. Loading of doxorubicin and thymoquinone with F2 gel nanofibers improves the antitumor activity and ameliorates doxorubicinassociated nephrotoxicity. Journal of Life Sciences. (2018) doi:10.1016/j.lfs.2018.06.008

[47] Sharbaf, F. G., Farhangi, H., & Assadi, F. Prevention of Chemotherapy-Induced Nephrotoxocity in Children with Cancer. International Journal of Preventive Medicine, 8(Oct), 76. (2017) Doi: 10.410/ijpvm.IJPVM_40_17

[48] Lee, H. H., Leake, B. F., Kim, R. B., & Jo, R. H. Contribution of Organic Anion-Transporting Polypeptides 1A/1B to Doxorubicin Uptake and Clearance. Molecular Pharmacology, 91(1), (2017)14-24. Doi: 10.1124/mol.116.105544

[49] El-Kenawi, A., Gatenbee, C., Robertson-Tessi, M., Bravo, R., Dhillon, J., Balagurunathan, Y., Berglund, A., Visvakarma, N., Ibrahim-Hashim, A., Choi, J., Luddy, K., Gatenby, R., Pilo-Thomas, S., Anderson, A., Ruffell, B., & Gillies, R. Acidity promotes tumour progression by altering macrophage phenotype in prostate cancer. British Journal of Cancer, 121(7), (2019)556-566. Doi: 10.1038/s41416-019-0542-2

[50] Yang, G., Wang, X., Fu, S., Tang, R., & Wang, J. pH- triggered chitosan nanogels via an ortho ester-based linkage for efficient chemotherapy. Acta Biomaterialia, 60(Sep), (2017) 232-243. Doi: 10.1016/j.actbio.2017.05.003